Control of thermal effects in fiber lasers by managing doping

A. TANDIROVIÇ GÜRSEL[a*], M. SADETTIN ÖZYAZICI[b*]
[a]*Department of Electrical and Electronics Engineering, University of Gaziantep, Gaziantep, 27310, Turkey*
[b]*Department of Electrical and Electronics Engineering, Bahçesehir University, Istanbul, 34353, Turkey*

Thermal load and non-linear effects put important limitations to the rapid progress of high-power fiber laser technologies. Thermal effect which limits the average power can be minimized by using low-doped, longer fibers with low gain, while the presence of non-linear effects requires the use of high-doped, shorter fibers in order to maximize the peak power. The proposed solution for the problem is to use varying doping levels along the short fiber to circumvent the trade-off between thermal load and non-linear effects. The study shows that two different approaches to mitigate the temperature levels above the intended temperature value.

(Received July 21, 2014; accepted January 21, 2015)

Keywords: Double-clad fiber lasers, Heat distribution, Absorption coefficient, Doping management

1. Introduction

Since 1960, when the first working laser was made by Maiman at Hughes Research Laboratories, the dynamic development of both host media and element laser transitions have brought about invention of a large variety of lasers. An important group of them is high-power fiber lasers (HPFL), which is one of the hot topics in the laser science and technology. In view of operating power, it can be said that the pioneering works were limited to sub-W levels [1-2] but strong demand for higher and higher power levels have led to the rapid progress of the technology and resulted in the development of multi-kilowatt ones [3-5]. Today, we cannot imagine the modern society without these unique light sources, for they have a large number of different applications in telecom [1], medicine [6], remote sensing, production technology [7], material processing [8], etc. due to many advantages such as better beam quality, high stability, low energy consumption, etc [1-10].

A common approach for higher laser efficiency is to increase the dopant concentration [3] which, unfortunately, also results in a higher absorption coefficient accompanied by the conversion of approximately 20% of pumping radiation into heat [11]. Although some studies have been considering a new technique intended to substantially reduce so-called waste heating [12-13], the main principle of which remains the same: desirable rise in average power levels drives up the thermal load in the fiber core that has adverse effects on the laser performance. Heating and beam-distorting effects are critical for high-power lasers [1-3]. Therefore, there is a great deal of interest in scaling the average power along with waste heating removal and thermal management [1].

For many reasons, thermal problems have been of a little concern for fiber lasers generating powers below 1kW [14]. For these lasers, thermal load was so small that the fiber wasn't actively cooled [15]. Heat and problem of thermal damage have been addressed since high power 1.5 μm signal was generated from short fiber cavity [14,16]. From the thermal point of view, it can be deduced that although many different kinds of cooling techniques are used the most influential way is the introduction of a particular cooling process for different wavelengths [17-19].

According to relevant researches, it can be said that the previous solutions focused on the diversification of the rare-earth-doped materials and monitoring their optical characteristics. As a result, Y_b-doped materials have come forward due to a variety of superior properties compared with the other counterparts [20-22]. Improvement in pumping diodes [9,23] and pumping technologies led to the evolution of the high gain fibers. An important step ahead was the invention of cladding pumping [8,24] or double-clad fiber lasers (DCFL's). In DCFL's the laser light propagates usually in a single-mode core, while the pump light is restricted to the core and multi-mode inner cladding by the lower refractive index of the outer cladding. DCFL's have two fundamental advantages: facilitated focusing and more homogenous pumping [11]. Likewise, a significant improvement has been achieved by breaking the cylindrical symmetry of the inner cladding [25]. Also, several geometries of the gain media, such as disc and slab as well as some specific geometrical shapes in charge of the thermal reduction, have been developed to overcome this limitation [8].

As noted before, a great deal in further scaling of DCFL's at kilowatt levels drove up to thermal analysis and calculations of internal thermal distribution have also become important issues as they could provide valuable information about the maximal expected temperature and thermal stress along the fiber [16]. Thus, they could avoid

irreversible damages inside the core as well as the polymer coatings of the fiber lasers since the materials used for low-index polymer coatings are very sensitive to high thermal loads especially when they are exposed for a long time. For long-term reliability operation below, 80 °C (253.1 K) may be required. The first numerical calculations were performed in 2-D frame which focused on transversal variation of thermal load ignored any change over the fiber length. However, as the fibers were shortened, increasing in deviations related to the thermal analysis that couldn't be neglected any more. For this reason, the importance and feasibility of the 3-D analysis was understood in a very short time.

There is no doubt that the foregoing methods are very important but it is also quite certain that the process will be limited along increasing of expected power levels. Therefore, it may be deduced that it is needed to find some complementary methods to take the heat under control. Herein, the doping management approach [5], revealed by Ilday and colleagues experimentally, but not theoretically, for 2 segments fiber which have different lengths but the same constant absorption coefficients, can be a promising method for further researches.

This study is a theoretical analysis of the doping management in with respect to thermal load, according to the thermal conductive equations that take the natural and geometrical properties of the fiber medium as well as the pump beam intensity profile into account.

2. Theoretical analysis of the heat distribution in double-clad fibers lasers

The temperature in fiber lasers is a 3-D boundary value problem, which is subjected to convective cooling, with the core acting as a heat source. The thermal conductivities of the double cladding materials are assumed to be the same since they are usually made of almost the same materials. Although there is some light intensity distribution in the inner cladding it can be neglected in the formulation since the inner cladding isn't doped and, as such, doesn't act as an energy source. Likewise no source is represented in the cladding region resulting in secondary effects of outer cladding that can be ignored. Hence, the inner and outer claddings can be considered as one body. A 3-D thermal distribution model for double-clad fiber is shown in Fig. 1. r is the radial coordinate, φ is the tangential angle, and z is the axial coordinate. The quantities $\boldsymbol{a}$ and $\boldsymbol{b}$ are core and cladding radii, respectively [16].

The steady-state heat equations for both core and cladding regions are given as follows [26-30]:

$$\frac{1}{r}\frac{\partial}{\partial r}\left(r\frac{\partial T_1(r,z)}{\partial r}\right)+\frac{\partial^2 T_1(r,z)}{\partial z^2}=-\frac{q(r,z)}{k_f};\quad 0\le r\le a \tag{1}$$

$$\frac{1}{r}\frac{\partial}{\partial r}\left(r\frac{\partial T_2(r,z)}{\partial r}\right)+\frac{\partial^2 T_2(r,z)}{\partial z^2}=0\,;\, a\le r\le b \tag{2}$$

It is to be notified that the azimuthal variation of the temperature is ignored due to the cylindrical symmetry of the fiber [22,26]. $T_1(r,z)$ and $T_2(r,z)$ are the temperatures in the core and cladding regions, respectively. In the equation (1) k_f denotes the thermal conductivity of the fiber core while $q(r,z)$ is the heat density given as a function of radius and propagation distance. For the forward pumped fiber laser with top-hat beam profile, which has a near-uniform energy density within a circular disk, the pumping distribution is given by:

$$P(z)=\xi P_O exp\left(-\alpha(z)z\right).$$

It is assumed that the heat generation of the rod has the same shape as the pumping light absorption [27]. So, the heat source density function can be represented as:

$$q\left(r,z\right)=\frac{\xi P_0}{\pi a^2 L_{eff}}\left(\alpha(z)+\alpha^{'}(z)z\right)exp\left(-\alpha(z)z\right) \tag{3}$$

Where $\boldsymbol{L_{eff}}$ is the effective length of the fiber given as: $L_{eff}=\left(1-exp\left(-\alpha(z)L\right)\right)/\alpha(z)$. P_o denotes the maximum pump power, $\alpha(z)$ is the pump absorption coefficient as variable of $\mathbf{z}$, ξ is the fractional thermal load or the conversion coefficient that appears due to the quantum defect [28].

In (2) the right side of the equation is zero as no source is represented. Temperature functions represented in (1) and (2) have to be solved using the method of separating variables with transformation $T(r,z)=\varphi(r)\theta(z)$. It takes into account that the temperature function has two separable components in radial and axial directions [19-20]. The differential equations to be solved are two separate differential equations with and without a source. The steady-state heat equations for both core and cladding regions are given as follows [27-31]:

$$\frac{1}{r\varphi_1(r)}\frac{\partial}{\partial r}\left(r\frac{\partial\varphi_1(r)}{\partial r}\right)+\frac{1}{\theta_1(z)}\frac{\partial^2\theta_1(z)}{\partial z}=-\frac{\xi P_0\left\{\alpha(z)+\alpha^{'}(z)z\right\}}{k_f\pi a^2 L_{eff}}\frac{exp(-\alpha(z)z)}{\varphi_1(r)\theta_1(z)} \tag{4}$$

$$\frac{1}{r\varphi_1(r)}\frac{\partial}{\partial r}\left(r\frac{\partial\varphi_1(r)}{\partial r}\right)+\frac{1}{\theta_1(z)}\frac{\partial^2\theta_1(z)}{\partial z}=0 \tag{5}$$

It is to be notified that both sides of equations (4) and (5) are divided by $\varphi(r)\theta(z)$.

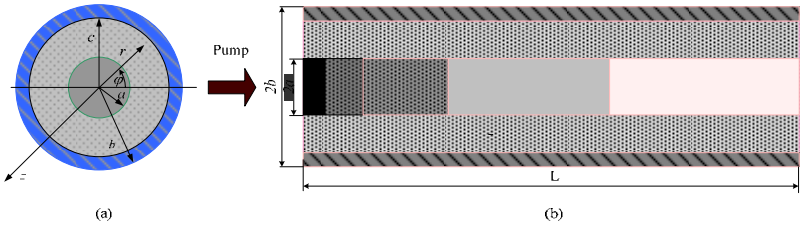

Fig. 1 Geometry of modeled double-clad fiber

As the absorption coefficient varies along z, the equation (4), as such, cannot be solved rigorously. The solution is possible if the whole fiber is considered as the set of n subsystems along the fiber axis each with a length L/n, where L is the total length of the fiber. For large values of n, all of those sub-systems act separately with the absorption coefficient can be treated as a constant. It is important to notify that, in terms of both power and temperature, the input of the each sub-system, except for the first one, is the output of the previous one. So, the pumping distribution of i-th sub-system, where $1 \leq i \leq n$ can be represented as:

$$P_i = P_{i-1} exp\left(-\alpha_i \frac{L}{n}\right) = P_0 exp\left(-\frac{L}{n}\sum_{j=1}^{i}\alpha_j\right) \tag{6}$$

Taking this property into account, the equations (4) and (5) can be re-written as:

$$\frac{1}{r\varphi_{1i}(r)}\frac{\partial}{\partial r}\left(r\frac{\partial\varphi_{1i}(r)}{\partial r}\right)+\frac{1}{\theta_{1i}(z)}\frac{\partial^2\theta_{1i}(z)}{\partial z}=-\frac{\xi P_i\alpha_i}{k_f\pi a^2}\frac{exp(-\alpha_i z)}{\varphi_{1i}(r)\theta_{1i}(z)} \tag{7}$$

$$\frac{1}{r\varphi_{2i}(r)}\frac{\partial}{\partial r}\left(r\frac{\partial\varphi_{2i}(r)}{\partial r}\right)+\frac{1}{\theta_{2i}(z)}\frac{\partial^2\theta_{2i}(z)}{\partial z}=0 \tag{8}$$

where $z_i = iL/n$.

For the axial parts represented in the exponential decay form $\theta_{1i}(z) = \exp(-\alpha_i z_i)$, $\theta_{2i}(z) = \exp(-\beta_i z_i)$, and $\eta_i = \xi P_i\alpha_i / k_f\pi a^2$ both equations are transformed into zero-order Bessel differential equations, which have the forms:

$$\frac{1}{r\varphi_{1i}(r)}\frac{\partial}{\partial r}\left(r\frac{\partial\varphi_{1i}(r)}{\partial r}\right)+\alpha_i^2=-\frac{\eta_i}{\varphi_{1i}(r)} \tag{9}$$

$$\frac{1}{r\varphi_{2i}(r)}\frac{\partial}{\partial r}\left(r\frac{\partial\varphi_{2i}(r)}{\partial r}\right)+\beta_i^2=0 \tag{10}$$

So, solutions for the radial parts of the temperature functions with and without a source are:

$$\varphi_{1i} = a_{1i}J_0(\alpha_i r)+a_{2i}Y_0(\alpha_i r)-\frac{\eta_i}{\alpha_i^2} \tag{11}$$

$$\varphi_{2i} = b_{1i}J_0(\beta_i r)+b_{2i}Y_0(\beta_i r) \tag{12}$$

Inasmuch as the temperatures of i-th sub-system are products of radial and axial parts, the functions can be represented as [18-19,27]:

$$T_{1i}(r,z_i)=\eta_i\left[A_{1i}J_0(\alpha_i r)-A_{2i}Y_0(\alpha_i r)-\frac{1}{\alpha_i^2}\right]\exp(-\alpha_i z)+Tc \tag{13}$$

$$T_{2i}(r,z_i)=\eta_i\left[B_{1i}J_0(\alpha_i r)-B_{2i}Y_0(\alpha_i r)\right]\exp(-\alpha_i z)+Tc \tag{14}$$

It is important to note that A_{2i} and B_{2i} are assumed to be negative. A_{1i}, A_{2i}, B_{1i}, and B_{2i} are arbitrary constants to be determined from boundary conditions given as:

$$T_1(r,z_i)\big|_{r=0} = finite \tag{15}$$

$$T_1(r,z_i)\big|_{r=a} = T_2(r,z_i)\big|_{r=a} \tag{16}$$

$$\int_V Q(r,z_i)dV = \int_S k_c\left.\frac{\partial T_2(r,z_i)}{\partial r}\right|_{r=b} dS \tag{17}$$

$$\left.\frac{\partial T_2(r,z_i)}{\partial r}\right|_{r=b} = \frac{h}{k_c}\left(T_c - T_2(r,z_i)\big|_{r=b}\right) \tag{18}$$

where k_c, T_c, and h are the cladding thermal conductivity, the cooling temperature, and the convective coefficient of the surface, respectively.

From the conditions (15) and (16), it is found that A_{2i} has to be zero as well as α_i=β_i . Hence, the relation between A_{1i} , B_{1i}, and B_{2i} can be expressed as:

$$A_{1i} = B_{1i} - B_{2i}\frac{Y_0(\alpha_i a)}{J_0(\alpha_i a)}+\frac{1}{J_0(\alpha_i a)\alpha_i^2} \tag{19}$$

Relation between B_{1i}, and B_{2i} can be obtained introducing the definition for derivative of the Bessel function in the condition (17):

$$B_{1i}J_1(\alpha_i b)-B_{2i}Y_1(\alpha_i b)=\frac{a^2}{2bK\alpha_i} \tag{20}$$

where $K = k_c/k_f$. Although in the most of the studies this ratio is considered to be 1, this study doesn't use this approximation.

From the condition (18), it is found out that:

$$B_{2i} = \frac{hJ_0(\alpha_i b) - k_c \alpha_i J_1(\alpha_i b)}{hY_0(\alpha_i b) - k_c \alpha_i Y_1(\alpha_i b)} B_{1i} \tag{21}$$

The equations (19), (20), and (21) form an equation set whose solutions are found to be:

$$A_{1i} = \frac{a^2 \left(J_0(\alpha_i a) - \gamma Y_0(\alpha_i a)\right)}{2bK\alpha_i J_0(\alpha_i a)\left(J_1(\alpha_i b) - \gamma Y_1(\alpha_i b)\right)} + \frac{1}{\alpha_i^2 J_0(\alpha_i a)} \tag{22}$$

$$B_{1i} = \frac{a^2}{2bK\alpha_i \left(J_1(\alpha_i b) - \gamma Y_1(\alpha_i b)\right)} \tag{23}$$

$$B_{2i} = \frac{a^2 \gamma}{2bK\alpha_i \left(J_1(\alpha_i b) - \gamma Y_1(\alpha_i b)\right)} \tag{24}$$

where $\gamma = \dfrac{hJ_0(\alpha_i b) - k_c \alpha_i J_1(\alpha_i b)}{hY_0(\alpha_i b) - k_c \alpha_i Y_1(\alpha_i b)}$

Using relations for cross-products of Bessel functions [31], the equations (23) and (24) form an equation set whose solutions are found to be:

$$B_{1i} = \frac{\pi a^2}{4bh}\left(hY_0(\alpha_i b) - k_c \alpha_i Y_1(\alpha_i b)\right) \tag{25}$$

$$B_{2i} = \frac{\pi a^2}{4bh}\left(hJ_0(\alpha_i b) - k_c \alpha_i J_1(\alpha_i b)\right) \tag{26}$$

Finally, using the equations (13, 14) and (22, 25, 26), 3-D analytical solutions for temperature distribution at core and clad regions with variable absorption coefficient, are obtained respectively as follows:

$$T_{1i}(r,z_i) = \frac{\xi\alpha_i}{k_f \pi a^2} P_0 exp\left(-\frac{L}{n}\sum_{j=1}^{i}\alpha_j\right) \times \times\left[\left(\frac{a^2\left(J_0(\alpha_i a) - \gamma Y_0(\alpha_i a)\right)}{2bK\alpha_i J_0(\alpha_i a)\left(J_1(\alpha_i b) - \gamma Y_1(\alpha_i b)\right)} + \frac{1}{\alpha_i^2 J_0(\alpha_i a)}\right) J_0(\alpha_i r) - \frac{1}{\alpha_i^2}\right] exp(-\alpha_i z_i) + Tc \tag{27}$$

$$T_{2i}(r,z_i) = \frac{\xi\alpha_i}{4bhk_f} P_0 exp\left(-\frac{L}{n}\sum_{j=1}^{i}\alpha_j\right) \times \times\left[\left(hY_0(\alpha_i b) - k_c\alpha_i Y_1(\alpha_i b)\right) J_0(\alpha_i r) - \left(hJ_0(\alpha_i b) - k_c\alpha_i J_1(\alpha_i b)\right) Y_0(\alpha_i r)\right] exp(-\alpha_i z_i) + Tc \tag{28}$$

The initial conditions for the heat in the core and cladding when z=0 can be found using 2-D analysis for double-clad fibers given in [27].

3. Results

The aim of this study is to prove that the variable absorption coefficient could keep the temperature constant or just suppress it along the fiber. On this basis, at first the numerical calculations were focused on verifying that the variable absorption coefficient can provide constant temperature function along the periphery of the fiber clad. Later the study was shifted on calculating and plotting the temperature functions for several generated absorption coefficient functions and comparing of the results in order to indicate the function that provides better suppress of the temperature. It is to be noted that the other fiber parameters are the same for all of the calculations and they are given as follows: l=2 m, *a*=20 µm, *b*=125 *µm*, k_c=23 W/mK, k_f=230 W/mK, P_o=150 W, Tc=300 K, h_c=50 W/m^{2}K, λ_p=976 nm, λ_L=1060 nm, and n=800.

For constant absorption coefficient calculations 3 different absorption coefficients have been used: α_1=0.4, α_2=0.1, and α_3=0.01. In order to take more precise information, the equations are numerically solved and plotted for both ***r=a*** and ***r=b*** using approximation by the first-degree spline function. One of these graphs is shown in Fig.2.a [32-34].

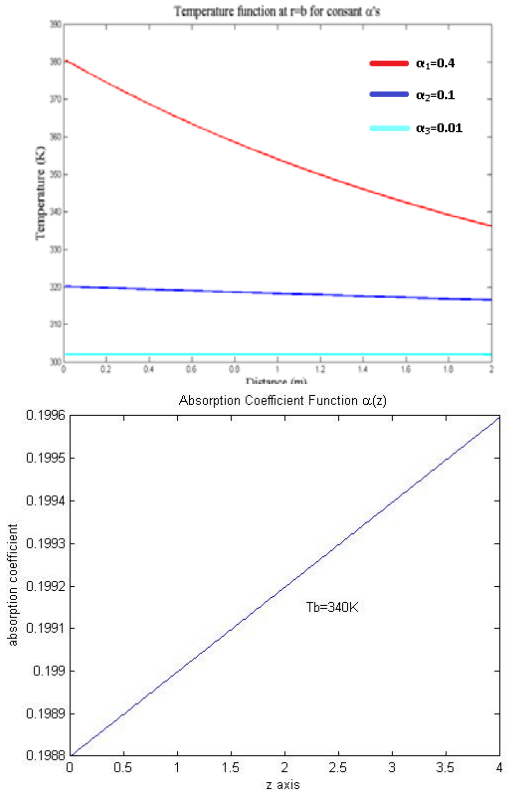

Fig.2.(a) Temperature distribution at r=b. (b) Absorption function along z axis at T_b=340K [32].

Fig.2.b is, in a sense, a proof that the temperature can be constant along the fiber and shows that it can be provided by slowly rise of the absorption coefficient along the z direction. That may encourage a more important discussion about the possibility of finding a more effective function or functions in terms of the temperature reduction.

Fig.3.a illustrates 3 different increasing absorption coefficient functions which rise between 0.01 and 0.4 [34], used for temperature calculations whose results are represented in Fig.3.b. The variable absorption coefficient functions, whose polynomial forms are represented below, were generated in order to ensure better suppression of the temperature along the fiber.

$$\alpha_1(z) = -0.0081z^5 + 0.0814z^4 - 0.1628z^3 + 0.1747z^2 - 0.0237z + 0.01 \quad (27)$$

$$\alpha_2(z) = 0.0326z^5 - 0.179z^4 + 0.4036z^3 - 0.5651z^2 - 0.6221z + 0.01 \quad (28)$$

$$\alpha_3(z) = 0.195z + 0.01 \quad (29)$$

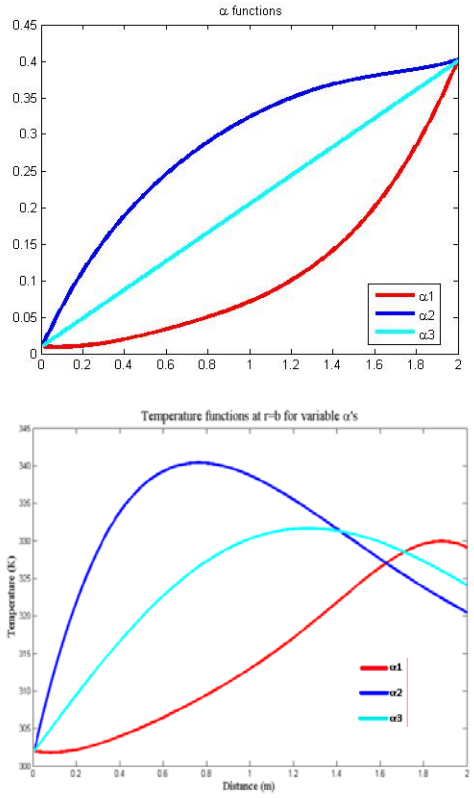

Fig.3.a-b Temperature distributions at r=b for 3 different polynomials.

4. Discussion

According to Fig. 2 it is quite certain that an increase of absorption coefficient brings about higher maximum temperature and it reaches at pumping side of the fiber laser. At the same time, higher absorption coefficient provides more significant drop in temperature along the fiber. On this basis, it can be deduced that some increasing absorption function can cause reduction in the temperature along the fiber [33].

In the light of this, it can be discussed about the possibility of keeping the $T_1(r,z)$ or $T_2(r,z)$ temperatures constant or holding the temperature under a certain value in the longitudinal direction the fiber. One of these studies is represented in Fig.2.b that shows absorption coefficient function via z axis necessary for keeping the temperature constant at $r=b$.

On the part of the non-linearity properties, especially for short length fibers, it may be more useful to opt for a repression of the temperatures under the certain values since better results have been achieved for shorter lengths. In order to support this opinion the absorption coefficient is represented in 3 different polynomial forms given in [33].

As can be seen from Fig.3.b gradual rise of the absorption coefficients results in gradual temperature increase. But, more important, all of the temperature functions with gradually raised absorption coefficient produce considerably smaller temperature rates than in the constant case, which verifies practical results presented by Elahi and colleagues [5]. Additionally, the best results are achieved for the first absorption coefficient function.

5. Conclusion

A heat dissipation model is given for double-clad fiber lasers with top-hat pump beam with cooling at the outer cladding surface. Also, the system has been numerically solved using 3-D heat transfer functions for variable absorption coefficient.

From the results of the analysis, the graphs are presented for both constant and variable absorption coefficients as well as absorption coefficient, which is a function of the temperature along z axis. The calculations do not only verify postulate proved experimentally by Elahi and colleagues but also show that the gradual rise of the absorption coefficient causes remarkable reduction in temperatures at core and clad of the fiber laser. In terms of thermal considerations, it can be said that the best results have been achieved for the first polynomial since the maximum achieved temperature is approximately 330K. It can be said that it is a significant reduction compared to the long-term reliability operation temperature, which is around 253.1 K. It is obvious that the temperature difference between the maximum achieved temperatures and the long-term reliability operation temperature may give also the chance to increase the final, maximum reached value of the variable absorption coefficient that can be an important step forward in power scaling that is restrained by the heat and problem of thermal damage.

The numerical results also show that longitude temperature variations cannot be neglected in the thermal analysis of any type of high-power fiber laser. Moreover, it can be introduced as an active part of thermal control

and may be helpful in avoiding devastating temperatures at fiber cores.

References

[1] J. Nilsson et al., Optical Fiber Communication Conference, 2005, paper OTuF1.

[2] J. Nilsson, Lasers and Electro-Optics (CLEO) and Quantum Electronics and Laser Science Conference (QELS), 2010, paper CTuC1.

[3] J. Nilsson, et al., SPIE Photonics West, Short Course, sc748 (2011).

[4] B. Zintzen , T. Langer , J. Geiger , D. Hoffmann, P. Loosen, SPIE 6873, Fiber Lasers V: Technology, Systems, and Applications, 2008, p.687319.

[5] P. Elahi1, S. Yılmaz, O. Akçaalan, H. Kalayıoğlu, B. Oktem, Ç . Şenel, F. Ö. Ilday, K. Eken, Optics Letters **37(**15), , 3042 (2012).

[6] J.A.Alvarez-Chavez, L.De La Cruz May, A. Martínez-Ríos, I. Torres-Gómez, Electronics and Photonics, 2006, p.279.

[7] A.Tunnermann, J. Limpert, and S. Nolte, Lasers and Electro-Optics, 2007 and the International Quantum Electronics Conference. CLEOE-IQEC 2007, Munich, 2007, p.1.

[8] H. R. Müller, J.Kirchhof, V.Reichel, & S.Unger, Comptes Rendus Physique, **7**(2), 154 (2006).

[9] D. J. Richardson, J. Nilsson, W. A. Clarkson, J., Optical Society of America B B **27**, B63 (2010).

[10] J. Nilsson, Y.Jeong, Codemard, C.Farrell, L.Ji, M. S. Z.Abidin, G. van der Westhuizen, S. Yoo, J. K. Sahu, Lasers and Electro-Optics 2009 and the European Quantum Electronics Conference. CLEO Europe-EQEC 2009 p. 1.

[11] A. Tunnermann, T Schreiber, F Röser, A.Liem, S. Höfer, H. Zellmer, S Nolte, J.Limpert, Journal Of Physıcs B: Atomıc, Molecular And Optıcal Physıcs **38**, 681 (2005).

[12] S. R. Bowman: "Lasers Without Internal Heat Generation", IEEE Journal of Quantum Electronics, **35(**1), 115 (1999).

[13] S.R. Bowman, S.P. O'Connor, S. Biswal, N.J. Condon, A. Rosenberg, IEEE Journal of Quantum Electronics, **46**(7), 1076 (2010).

[14] L. Li, H. Li, T. Qiu, V. L. Temyanko, M. M. Morrell, A. Schülzgen, Optical Society of America, Optics Express **13(**9), 3420 (2005).

[15] J. K. Sahu, Y. Jeong, D. J.Richardson, & J. Nilsson, Optics communications, **227**, 159 (2003).

[16] D.C Brown. Hanna J. Hoffman, IEEE Journal of Quantum Electronic **37**(2), 207 (2001).

[17] K. Ueda, "High Power Fiber Lasers". CLEO/ Pacific Rim 4th Conference of Lasers and Electro-Optics, 2001, p.2.

[18] V. Ashoori, A. Malakzadeh, Journal of Physics D: Applied Physics **44**. 35 (2011).

[19] N. K. Salim , An Overview of Heat Transfer Phenomena, InTech, 2012.

[20] Jeong, Yoonchan, et al. , Opto-Electronics and Communications Conference (OECC), 2012 17th. IEEE, Busan Korea 2012, p.580

[21] J. Kirchhof, S. Unger, A. Schwuchow, Journal of Non-Crystalline Solids, **352**, 2399 (2006).

[22] T. C. Newell, P. Peterson, A. Gavrielides. M. P. Sharma, Journal Optics Communications, Optical Society of America, **273**, 256 (2007).

[23] X. Liu, Y. Wang, J. Wang, E. Zhang, L. Xiong, W. Zhao, The Pacific Rim Conference on Lasers and Electro-Optics 2009, IEEE, CLEO/PACIFIC RIM'09, 2009, p. 1.

[24] Y.Jeong, et. al., In Communications and Photonics Conference and Exhibition (ACP), 2010 Asia, Shanghai. 2010, p.381.

[25] P. Konieczny, J. Świderski, A. Zajač, M.Skórczakowski, Optica Applicata, **35(**4), 955 (2005).

[26] J.Li, K. Duan, Y. Wang, Journal of Modern Optics, **55(**3), (2007).

[27] M. E. H. Assad, D. C. Brown, IEEE Journal of Quantum Electronic **49(**1), 100 (2013).

[28] D. Xue, Fiber Lasers, Optics **122**, 932 (2010).

[29] P. Li, C. Zhu, S. Zou, Optics and Laser Technology, **40237**, 360 (2008).

[30] G. Canat, Y. Jaouën , Optics Letters, **30(**22), 3030 (2005).

[31] E.T. Goowin, Oxford Journals Quarterly Jnl. of Mechanics & App. Maths. **2**(1),73 (1948).

[32] A. Gürsel Tandiroviç, P. Elahi, F. Ö. İlday, M.S. Özyazıcı, FOTONİK 2013, 2013, p.14.

[33] A. Gürsel Tandiroviç, P. Elahi, F. Ö. İlday, M.S. Özyazıcı, 8th International Conference on Electrical and Electronics Engineering ELECO 2013, 2013.

[34] A. Gürsel Tandiroviç, P. Elahi, F. Ö. İlday, M.S. Özyazıcı, Turkish Journal of Electrical Engineering & Computer Science,**1402,** 239 (2014).

*Corresponding author: gursel@gantep.edu.tr , sadettin.ozyazici@bahcesehir.edu.tr